



HAL
open science

Sequential detection of a total instantaneous blockage occurred in a single subassembly of a sodium-cooled fast reactor

Igor V. Nikiforov, Fouzi Harrou, Rémi Cogranne, Pierre Beuseroy, Edith Grall-Maës, Blaise Kévin Guépié, Lionel Fillatre, Jean-Philippe Jeannot

► To cite this version:

Igor V. Nikiforov, Fouzi Harrou, Rémi Cogranne, Pierre Beuseroy, Edith Grall-Maës, et al.. Sequential detection of a total instantaneous blockage occurred in a single subassembly of a sodium-cooled fast reactor. Nuclear Engineering and Design, 2020, 366, pp.110733. 10.1016/j.nucengdes.2020.110733 . hal-02906760

HAL Id: hal-02906760

<https://hal.science/hal-02906760v1>

Submitted on 18 Jul 2022

HAL is a multi-disciplinary open access archive for the deposit and dissemination of scientific research documents, whether they are published or not. The documents may come from teaching and research institutions in France or abroad, or from public or private research centers.

L'archive ouverte pluridisciplinaire **HAL**, est destinée au dépôt et à la diffusion de documents scientifiques de niveau recherche, publiés ou non, émanant des établissements d'enseignement et de recherche français ou étrangers, des laboratoires publics ou privés.



Distributed under a Creative Commons Attribution - NonCommercial 4.0 International License

Sequential detection of a total instantaneous blockage occurred in a single subassembly of a sodium-cooled fast reactor

Igor Nikiforov ^{*}, Fouzi Harrou ¹, Rémi Cogranne, Pierre Beuseroy, Edith Grall, Blaise Kevin Guépié, Lionel Fillatre ²

UTT/ICD/LM2S, FRE CNRS, Université de Technologie de Troyes, 12, rue Marie Curie CS 42060 10004 Troyes Cedex, France

Jean-Philippe Jeannot

CEA, DEN/CAD/DTN/STCP/LISM, Commissariat à l'Energie Atomique et aux Energies Alternatives, Bâtiment 202, 13108 Saint-Paul-lez-Durance, France

Abstract

The on-line diagnosis can be defined as a sequence of operations designed to detect, to isolate an anomaly and to mitigate its impact before it affects the inspected system. In the context of the project ALPES 2 (local accidents – protection and monitoring, in English) of the GIS 3SGS (group of scientific interest – surveillance, dependability, security of large systems, in English), the statistical methods for the early detection of a Total Instantaneous Blockage (TIB) occurred in a single subassembly of a sodium-cooled fast reactor have been studied. This work is carried out within the framework of model-based detection methods. The goal of this paper is to study the feasibility of a sequential approach to detect an abnormal local temperature rise of neighboring subassemblies due to a TIB while respecting the probability of missed detection, the probability of false alarm and the required time-to-alert. The adaptive statistical estimation/detection method is based on the measurements taken from ThermoCouples (TCs) located above the subassemblies. The aim is therefore to provide a complementary tool to improve the early detection of a TIB in the context of nuclear safety.

Keywords: Nuclear safety, Sodium fast reactor, Subassembly total instantaneous blockage, Core outlet sodium temperature, Model-based statistical detection, Transient changes.

^{*}Corresponding author. *Email address* : nikiforov@utt.fr

¹F. Harrou is now with the Computer, Electrical and Mathematical Sciences and Engineering (CEMSE) Division, King Abdullah University of Science and Technology (KAUST), Thuwal, Saudi Arabia.

²L. Fillatre is now with the Université Côte d'Azur, CNRS, I3S Laboratory - UMR 7271 - CS 40121 - 06903 Sophia Antipolis Cedex, France.

Nomenclature

Symbol	Description
Y_t	vector of observations, outlet temperatures ($^{\circ}\text{C}$) at discrete time t , $Y_t \in \mathbb{R}^n$
n	number of thermocouples in a group
ΔT	sampling period in seconds (s)
p_t	core thermal power at discrete time t (megawatt)
\tilde{X}	vector of regression coefficients, $\tilde{X}_t \in \mathbb{R}^{\ell}$
ℓ	number of regressors
p	order of the autoregressive model with exogenous inputs
(u_i, v_i)	sensor (thermocouple) position, $i = 1, \dots, n$
A_i	the i -th matrix of autoregressive coefficients, $i = 1, \dots, p$
\tilde{H}_t	regression matrix of size $n \times \ell$ at discrete time t
$\{\xi_t\}_{t \geq 1}$	sequence of outlet temperature one-step prediction errors ($^{\circ}\text{C}$), $\xi_t \in \mathbb{R}^n$
σ_i	the i -th standard deviation of the component $\xi_{t,i}$ ($^{\circ}\text{C}$)
$\{\varepsilon_t\}_{t \geq p+1}$	sequence of model residuals ($^{\circ}\text{C}$), $\varepsilon_t \in \mathbb{R}^n$
$\hat{\sigma}_i$	the i -th empirical standard deviation of the component $\varepsilon_{t,i}$ ($^{\circ}\text{C}$)
t_0	TIB arrival time (“change-point”) measured in discrete time
N	required time-to-alert measured in discrete time
m_{α}	reference period measured in discrete time
T_{FMA}	discrete time of TIB detection (stopping time of the FMA test)
$\overline{\mathbb{P}}_{\text{md}}(T)$	the worst-case probability of missed detection
$\overline{\mathbb{P}}_{\text{fa}}(T; m_{\alpha})$	the worst-case probability of false alarm during the reference period m_{α}
Abbreviations	
ACF	AutoCorrelation Function
ARL	Average Run Length
ARX	AutoRegressive model with eXogenous inputs
CDF	Cumulative Distribution Function
FMA	Finite Moving Average
LLR	Log-Likelihood Ratio
LS	Least Squares
MW	MegaWatt
PDF	Probability Density Function
RLS	Recursive Least Squares
SFR	Sodium Fast Reactor
TC	ThermoCouple
TIB	Total Instantaneous Blockage
TRL	Technological Readiness Level

1. Introduction and motivation

Online monitoring of critical industrial systems, such as nuclear reactors, plays an important role in improving their safety and productivity. Furthermore, early fault detection and isolation are vital to maintaining reliable process operation and avoiding

expensive maintenance. For instance, the Fukushima accident of 2011 in Japan revealed the highest need for developing accurate and efficient monitoring systems for nuclear plants. Accordingly, this paper focuses on designing an innovative statistical monitoring technique for enhancing nuclear reactor safety.

The central core of Sodium Fast Reactor (SFR) contains the fuel subassemblies bundled in a rectangular or hexagonal array. The fuel elements, called fuel pins (or fuel rods), are formed of a stack of fissile fuel pellets placed in thin cylindrical steel tubes and closed by welding of end plugs at both the ends. The fuel rods are then grouped into subassemblies (see Figure 1). The subassemblies ensure the channelization of the coolant flow that cools the fuel pins. The heat produced by the nuclear reaction is evacuated by the liquid coolant circulating between the fuel pins and in the clearance between the subassemblies. In the case of SFR, the liquid coolant used is sodium in the liquid state. It flows in a closed circuit from the bottom of the subassembly upward through pumps. One or more heat exchangers are provided at the outlet of the assembly for extracting heat from the coolant. Since the fuel pins are closely packed in the central core of SFR, the space between them is kept to a minimum value by using spiral spacer wires placed across the fuel pin in the axial direction [1, 2].

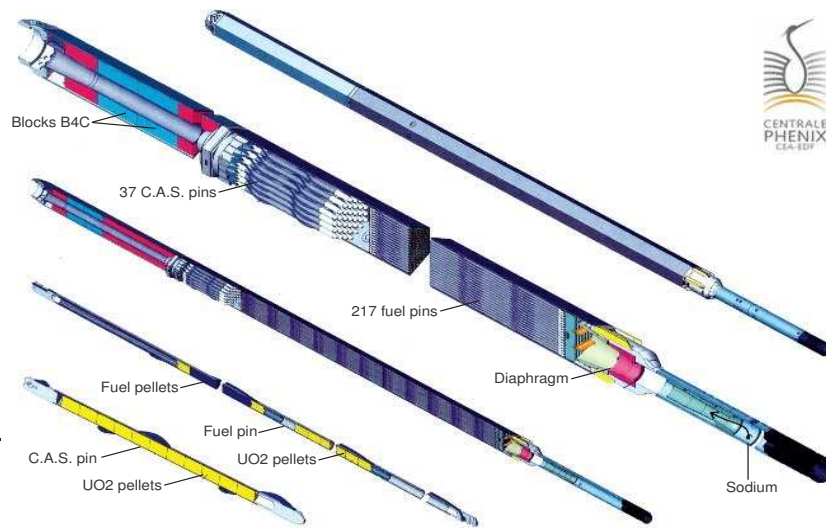


Fig. 1. Fuel assembly of the French SFR "Phénix".

In the safety approach for the core of the 4-th generation French SFR, the TIB is a hypothetical accident scenario belonging to a prevention situation category (probability inferior to 10^{-6} per year). This scenario is very unlikely as it assumes a complete and simultaneous blockage of all the subassembly inlet ports when the reactor is at full power. However, the study of a single subassembly inlet port blockage is justified because it is considered as a limiting accident [3, 4]. As it follows from [4], the TIB

30 formation in a subassembly contained a fuel pin could be initiated by various possible ways such as loading of blocked subassemblies, passing of foreign particles such as weld spatter present in primary circuit through core via coolant, clogging by broken spacer wire, etc.

This paper is devoted to the sequential (on-line) statistical detection of a TIB occurred in a single subassembly by detecting an abnormal temperature rise with the TCs at the top of the fuel subassemblies that monitor the neighboring subassemblies. This temperature rise is a consequence of the heating of adjacent subassemblies by conduction through the hexcans. Because the inlet port blockage, the temperature measured above the subassembly with a TIB is not representative for the TIB detection. The early detection of an abnormal temperature rise provoked by a TIB has been previously considered in [5, 6, 7]. The recursive filtering based on the statistical estimation theory is used to reduce the outlet temperatures uncertainties in [5]. Next, the filtered TCs signals are used to detect a local temperature rise due to a TIB. The TIB detection algorithms based on the artificial neural network-based strategies are used in [6, 7].
45 Nevertheless, some problems hold unsolved, especially, the calculation of the probabilities of missed detection and false alarm. These probabilities are crucially important to estimate the Technological Readiness Level (TRL) for the early TIB detection based on the core outlet temperatures.

The proposed TIB detection algorithm is composed of two parts. The first part is an adaptive estimation of the stochastic-dynamic model of subassembly outlet temperatures. This model is used to generate the residuals sensitive with respect to (w.r.t.) the abnormal temperature rise due to a TIB and, simultaneously, insensitive w.r.t. normal operating temperature variations. The second part is the statistical sequential test, which uses the residuals generated by the stochastic-dynamic model of subassembly outlet temperatures to detect the temperature rise due to a TIB.
55

The original contributions of this paper are as follows :

- The detection of an abnormal temperature rise due to a TIB is reduced to the problem of reliable detection of transient changes in the temperature signals by using a parametric model of the subassembly outlet temperature.
- 60 • The Finite Moving Average (FMA) test for a reliable detection of a TIB is combined with the recursive adaptive Least Squares (LS) estimator. This LS estimator is used to reduce a negative impact of the outlet temperatures uncertainties on the FMA test.
- In contrast to the previous publications, the asymptotic upper bounds for the probabilities of missed detection and false alarm are proposed in the current paper. These upper bounds permit to predict the statistical properties of the proposed solution.
65
- The performance of the proposed FMA test has been evaluated with records of normal operating outlet temperatures collected on the French SFR “Phénix” by

70 the CEA. The abnormal temperature rise in the neighboring subassemblies has been simulated.

This paper is organized as follows. Section 2 states the problem of a TIB detection. The temperature records from the TCs above the subassemblies used for this study are presented in Section 3. These records provided to us by the CEA, Cadarache. Next, 75 an explanatory parametric model describing the subassembly outlet temperature is developed in Section 4. This parametric model is non-stationary. An adaptive parameter estimation algorithm is proposed in Section 5. The reliable detection of transient changes, the nuisance parameter rejection and the design of the FMA test combined with an adaptive estimator are discussed in Section 6. The statistical properties of the 80 detector and its evaluation with real data are also discussed in Section 6. Finally, some conclusions are drawn in section 7.

2. The TIB of a subassembly

The subassembly plays an essentially hydraulic role. It guarantees the channelization of the sodium flow, which cools the fuel pins. Following a TIB, the subassembly 85 is cooled only by the “inter-assembly” sodium flow and the sodium contained in the subassembly very quickly reaches the vaporization temperature. After evaporation of the sodium, the steel tubes of the fuel pins melt and partially solidify in the bottom of the assembly remained cold. The fuel pellets then reach the melting temperature and form a molten bath placed above the steel of the tubes. Lateral cooling by inter- 90 assembly sodium flow results in the formation of a solid fuel crust along the hexagonal steel casing that temporarily prevents its melting [8]. The rest of the incident depends essentially on the existence of a plug in the upper part of the assembly. At the time of melting the fuel pellets, it is highly likely that the fission gases thus released cause molten material to the top of the assembly. As a result of their re-solidification a plug, 95 possibly porous, could be formed.

Several methods of a TIB early detection for the 4-th generation French SFR are considered in [3]. As it follows from [3], the highest TRL can be attributed to the method of early detection based on the core outlet temperatures collected from the TCs above the individual subassemblies. The outlet temperature is a permanently monitored parameter for obvious safety reasons. The temperature measurements at the top 100 of the fuel subassemblies allow the operator to permanently have a map of the radial distribution of temperature output core. In the French concepts (“Phénix” and “Superphénix”), the core outlet sodium temperature is monitored by TC located inside a thimble (thermowell) above each subassembly [3]. The TIB of a subassembly causes 105 a rise in temperature of the heat transfer fluid of neighboring subassemblies while the temperature measured above the subassembly with a TIB is not representative for its detection because the inlet port blockage.

The principle of the early TIB detection based on the core outlet temperatures is to detect an abnormal temperature rise with the TCs that monitor the neighboring sub-assemblies. This temperature rise is a consequence of the heating of adjacent sub-assemblies by conduction through the hexcans. It has been estimated that this heating resulted in an increase of the neighboring outlet temperatures of a few tenths of °C/s per second for 10 s (until the hexcans rupture).

Up to our knowledge, the very first recursive filtering method to reduce the outlet temperatures uncertainties based on the statistical estimation theory has been proposed and tested with real data in [5]. The filtered signals used to detect a local temperature rise by using a rather rudimentary algorithm. The current paper can be seen as a further development of the method proposed in [5] by using the modern adaptive statistical estimation and detection algorithms based on the temperature measurements from the TCs located above the subassemblies. This involves studying the sensitivity of TCs for the detection of a local temperature rise of at least two neighboring subassemblies while respecting the probability of non-detection, the probability of false alarm and the maximum detection delay. The early detection of the TIB makes it possible to prevent the propagation of this fusion to the entire active core, i.e. adjacent assemblies, which could result in the destruction of the reactor envelope, or even the containment of reactor.

3. Real data used in this study

The temperature measurements used in this study come from the French SFR “Phénix”(today at final shutdown). They were collected in 2009 during the end-of-life tests of the plant. These data were provided by the center of the CEA in Cadarache. The core outlet temperatures have been collected from the TCs, placed into the control plug for real-time observation of sodium outlet temperatures from individual subassemblies. The data acquisition system has been equipped with a 8-bit analog-to-digital converter. The spatial distribution of TCs in the core is illustrated in Figure 2(a).

For this study, we have used the dataset containing the temperature measurements from 121 TCs located above the centers of the subassemblies shown in Figure 2(a). The TCs provide the temperature measurement every three seconds, i.e. the sampling period is $\Delta T = 3$ s. This dataset is composed of two samples covering two periods. The first sample covers a 7-day period from 15/02/2009 to 21/02/2009. The second sample covers a second 7-day period from 01/03/2009 to 07/03/2009. The sample sizes are 201587 and 173882 observations, respectively. Moreover, two samples of the core thermal power synchronized with the two above-mentioned periods have been also used.

The instantaneous temperature field measured at the positions (u_i, v_i) , $i = 1, \dots, 121$, is represented in Figure 2(b). First of all, it is worth noting that the spatial distribution of the temperature is not symmetrical. We can also notice that the temperature is more important in the center than on the edges. The average temperature in the

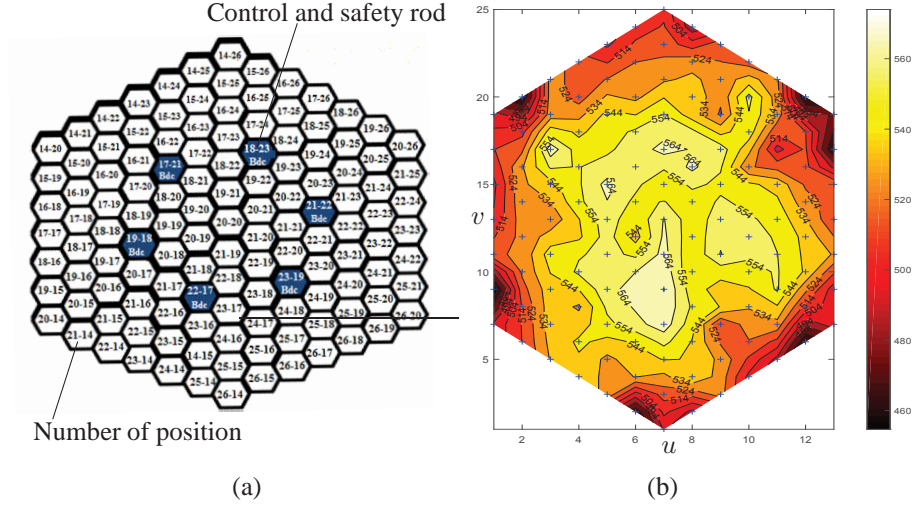


Fig. 2. **a)** The assembly of 121 fuel rods. **b)** The instantaneous temperature field measured in $^{\circ}\text{C}$. Blue crosses indicate the positions (u_i, v_i) of TC. Black numbers indicate the temperatures in $^{\circ}\text{C}$ corresponding to the level curves.

center is approximately equal to 560°C and 460°C in the periphery. The temperatures do not vary in a homogeneous way over the whole core. Since the behavior of the temperature depends on the position of the TC, it seems appropriate to take into account the positions of the TCs to describe the evolution of the temperature.

In the following, we will try to build a model that describes the variations of temperature signals in the absence of local temperature increase associated with a TIB.

4. Nominal model of the subassembly outlet temperature

This section is devoted to a stochastic-dynamic model of subassembly outlet temperatures measured by a small group of neighboring TCs under normal operating conditions (without a TIB). The goal of this model is to define a projection of the observed data on a specially designed subspace, free from the normal operating variations of the outlet temperatures vector $Y \in \mathbb{R}^n$ measured each ΔT seconds at the positions (u_i, v_i) , $i = 1, \dots, n$.

From the preliminary data analysis, it has been established that an adequate description of the local temperature field can be done by the AutoRegressive Moving – Average model with eXogenous inputs, i.e. ARMAX (p, q) model, where p is the order of the AR part and q is the order of the MA part. In the sequel, our attention is restricted to a subclass of ARMAX (p, q) model, i.e. to the AutoRegressive model with eXogenous inputs ARX (p) model. There are two reasons for this :

- Despite the fact that the ARMAX (p, q) model is more flexible than the ARX (p) model, the parameter estimation in the case of ARMAX (p, q) model leads to a nonlinear minimization problem with the upper bound for the number of local minima comparable to the sample size. Adaptive parameter estimation in the case of ARMAX (p, q) model is even a more difficult problem because the effective sample size is constant. Hence, the probability to reach a wrong minimum is positive. In contrast to the ARMAX (p, q) model, the parameter estimation in the case of ARX (p) model is reduced to a quadratic minimization problem (with a single minimum). It can be easily solved by using a conventional recursive LS algorithm.
- The approximation of the MA polynomial $(1 - \sum_{i=1}^q B^i \beta_i)$ of order q by an AR polynomial $(1 - \sum_{i=1}^{\tilde{p}} B^i \alpha_i)$ of suitably high order \tilde{p} is frequently used

$$1 - \sum_{i=1}^q B^i \beta_i \simeq \frac{1}{1 - \sum_{i=1}^{\tilde{p}} B^i \alpha_i}, \quad \tilde{p} \gg q \quad (1)$$

where B^i is the operator of the delay (backshift operator): $B^i Y_t = Y_{t-i}$. Hence, the ARX (p) , $p = \tilde{p} + p_1$, model can be used as an approximation of the ARMAX (p_1, q) model.

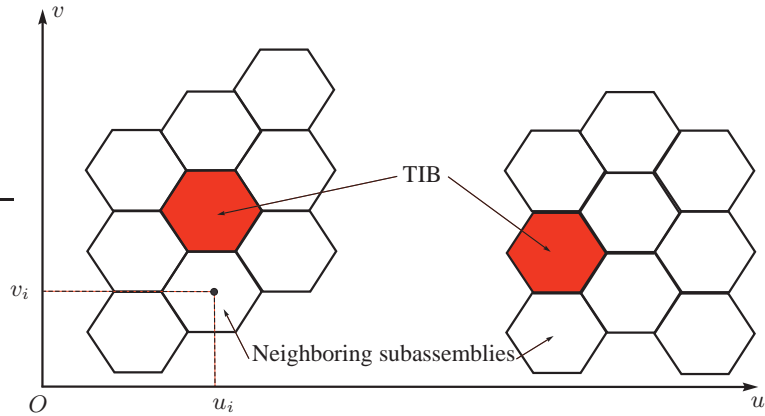


Fig. 3. Representation of two groups with 9 TCs : a potentially accidental subassembly (TIB) with its neighboring subassemblies.

Let us consider that a group of TCs, i.e. a potentially accidental subassembly (TIB) with its neighbors, is composed of n sensors installed at the positions (u_i, v_i) , $i = 1, \dots, n$. This situation is represented in Figure 3. We consider that the scalar temperature field Y measured each ΔT seconds at the positions (u_i, v_i) , $i = 1, \dots, n$, is

locally modeled by the following dynamic-stochastic ARX (p) equation [9, 10, 11]

$$\tilde{Y}_t = \left(I_n - \sum_{i=1}^p B^i A_i \right) Y_t = \tilde{H}_t \tilde{X} + \xi_t, \quad t = 1, 2, \dots, T \quad (2)$$

180 where $Y_t = (y_{t,1}, \dots, y_{t,n})^T \in \mathbb{R}^n$ is the vector of observations (temperatures) of n TCs at the discrete time instant t , I_n is the identity ($n \times n$) matrix $\tilde{H}_t \tilde{X}$ is a exogenous inputs term, which is used to model the behavior of the instantaneous scalar field of temperatures, $\tilde{X} \in \mathbb{R}^\ell$ is the vector of the unknown inputs (regressors), $(1 - \sum_{i=1}^p B^i A_i)$ is the AR polynomial of order p , $A_i = \text{diag}\{\alpha_{i,1}, \dots, \alpha_{i,n}\}$ is a diagonal ($n \times n$) matrix of AR coefficients, $\alpha_{i,j}$ is the AR coefficient, $\{\xi_t\}_{t \geq 1} \in \mathbb{R}^n$ is a sequence of i.i.d. random vectors from a zero-mean Gaussian distribution $\mathcal{N}(0, \Sigma)$, $\Sigma = \text{diag}\{\sigma_1^2, \dots, \sigma_n^2\}$.

Let us discuss the main elements of the ARX (p) model given by (2). The role of the linear explanatory term with exogenous inputs is to model the instantaneous behavior of the temperature field

$$\tilde{Y}_t = \tilde{H}_t \tilde{X} + \xi_t, \quad t = 1, 2, \dots, T \quad (3)$$

where $\tilde{Y}_t = (I_n - \sum_{i=1}^p B^i A_i) Y_t$ is the filtered vector of temperatures. To describe the temperature field, a polynomial in u and v has been chosen. Hence, the filtered temperature $\tilde{y}_{t,i}$ measured by the TC i located in the position (u_i, v_i) at time t is given by

$$\tilde{y}_{t,i} = \tilde{h}_{t,i} \tilde{X} + \xi_{t,i} = \sum_{k=0}^2 \sum_{m=0}^2 u_i^m v_i^k a_{m,k} + p_t b + \xi_{t,i}, \quad i = 1, \dots, n \quad (4)$$

where p_t is the core thermal power at time t measured in megawatt (MW) and the row vector $\tilde{h}_{t,i}$ of matrix \tilde{H}_t is given by

$$\tilde{h}_{t,i} = (u_i^2 v_i^2, u_i v_i^2, v_i^2, u_i^2 v_i, u_i v_i, v_i, u_i^2, u_i, 1, p_t), \quad i = 1, \dots, n$$

The vector $\tilde{X} \in \mathbb{R}^\ell$, where $\ell = 10$, represents the unknown nuisance parameters composed of the polynomial coefficients and the coefficient of the core thermal power. The first 9 coefficients of the vector

$$\tilde{X} = (a_{2,2}, a_{1,2}, a_{0,2}, a_{2,1}, a_{1,1}, a_{0,1}, a_{2,0}, a_{1,0}, a_{0,0}, b)^T$$

180 reflect the geometric factors (spatial correlation between neighboring TCs) and the coefficient b reflect the impact of the core thermal power. The matrix \tilde{H}_t of size $(n \times 10)$ is composed of n rows $\tilde{h}_{t,i}$, $i = 1, \dots, n$.

Discussion. At first glance, it may seem strange that the last two columns coexist in the matrix \tilde{H}_t . But it is worth noting that the roles of the last two columns in the matrix \tilde{H}_t are different. The ninth column defining the common factor of the polynomial approximation for the temperature field in the core. It is responsible, together with the first 8

195 columns, for the best possible instantaneous fitting of this polynomial approximation
to the temperature field. The tenth column is responsible for the linear relationship
between the outlet temperatures and the core thermal power, which can rapidly vary
between the minimum and maximum values as it happens in the case of the second 7-
day period from 01/03/2009 to 07/03/2009. The coefficients $a_{0,0}$ and b of the vector \tilde{X}
200 have quite different dynamics (see Figures 8(a) and 9(a)). This coexistence improves
the quality of the ARX (p) model given by (2), especially for the second 7-day period
from 01/03/2009 to 07/03/2009.

Therefore, the right-hand side of the ARX (p) model given by (2) represents a
combination of the regressive part defined by the term $\tilde{H}_t X$ and the AR part defined
by the term $\sum_{i=1}^p A_i Y_{t-i}$. Equations (2) and (4) can be re-written in the vector form
as follows

$$Y_t = \tilde{H}_t \tilde{X} + \sum_{i=1}^p A_i Y_{t-i} + \xi_t, \quad t = 1, 2, \dots, T \quad (5)$$

and in the scalar form

$$y_{t,i} = \sum_{k=0}^2 \sum_{m=0}^2 u_i^m v_i^k a_{m,k} + p_t b + \sum_{j=1}^p \alpha_{j,i} y_{t-j,i} + \xi_{t,i}, \quad i = 1, \dots, n, \quad t = 1, 2, \dots, T \quad (6)$$

The traditional method of the ARX model estimation is to re-write the above equations
(5) and (6) in the form of regression model (see [10])

$$\underbrace{\begin{pmatrix} Y_t \\ y_{t,1} \\ \vdots \\ y_{t,i} \\ \vdots \\ y_{t,n} \end{pmatrix}} = \underbrace{\begin{pmatrix} \tilde{H}_t & y_{t-1,1} & \dots & y_{t-p,1} & \dots & 0 & \dots & 0 \\ \vdots & \vdots & \dots & \vdots & \dots & \vdots & \dots & \vdots \\ 0 & \dots & \dots & 0 & \dots & 0 & \dots & 0 \\ \vdots & \vdots & \dots & \vdots & \dots & \vdots & \dots & \vdots \\ 0 & \dots & \dots & 0 & \dots & y_{t-1,n} & \dots & y_{t-p,n} \end{pmatrix}}_{H_t} \underbrace{\begin{pmatrix} X \\ \tilde{X} \\ \alpha_{1,1} \\ \vdots \\ \alpha_{p,1} \\ \vdots \\ \alpha_{1,n} \\ \vdots \\ \alpha_{p,n} \end{pmatrix}} + \underbrace{\begin{pmatrix} \xi_t \\ \xi_{t,1} \\ \vdots \\ \xi_{t,n} \end{pmatrix}} \quad (7)$$

where $t = 1, 2, \dots, T$ and X is a vector of unknown parameters of size $q = \ell + np$.
It consists of two sub-vectors. The sub-vector \tilde{X} of size ℓ represents the regres-
sion (exogenous) parameters and the sub-vector $(\alpha_{1,1} \dots, \alpha_{p,1} \dots \alpha_{1,n} \dots, \alpha_{p,n})^T$ of
size np represents the AR parameters. Therefore, after elapsed time T , the total re-
gression model is defined by the following equation with the vectors $Y_{1,T} \in \mathbb{R}^{nT}$
(resp. $\xi_{1,T} \in \mathbb{R}^{nT}$) formed from the vectors Y_1, \dots, Y_T (resp. ξ_1, \dots, ξ_T) stacked
together and the matrix $H_{1,T}$ of size $(nT \times \ell + np)$ formed from the matrices

$H_t = H_t(\tilde{H}_t, Y_{t-1}, \dots, Y_{t-p})$, $t = 1, \dots, T$, stacked together

$$Y_{1,T} = \begin{pmatrix} Y_1 \\ \vdots \\ Y_T \end{pmatrix} = \begin{pmatrix} H_1 \\ \vdots \\ H_T \end{pmatrix} X + \begin{pmatrix} \xi_1 \\ \vdots \\ \xi_T \end{pmatrix} = H_{1,T} X + \xi_{1,T} \quad (8)$$

5. Adaptive estimation of the outlet temperature model

This section is devoted to the identification of the subassembly outlet temperature model given by (7) – (8) under normal operating conditions (without a TIB). In the case of time-invariant systems, the statistical properties of the LS estimation for the ARX (p) model have been studied in [9, 10, 11]. It has been shown that the ARX (p) model is reduced to a conventional regression model. Hence, it possesses all optimal properties of a linear regression (at least asymptotically, when $T \rightarrow \infty$). It is assumed that the covariance matrix of the random noise $\xi_{1,T} \in \mathbb{R}^{nT}$ is scalar, i.e. $\sigma_1^2 = \dots = \sigma_n^2$ and $\text{cov}(\xi_{1,T}) = \sigma^2 I_{nT}$. There are two reasons for this : *i*) all the outlet temperatures are measured by the same K-type TCs and these temperatures belong to the same interval, i.e. all the TCs have approximately the same Standard Deviation (SD) σ_i of instrumental errors; *ii*) the heteroscedasticity has no negative impact on the detection algorithm (see details in Section 6.2). Hence, the LS estimation and its residual vector are given by using the batch of T data

$$\hat{X} = (H_{1,T}^T H_{1,T})^{-1} H_{1,T}^T Y_{1,T}, \quad \Psi_{1,T} = P_{H_{1,T}} Y_{1,T} = Y_{1,T} - H_{1,T} \hat{X} \quad (9)$$

where $\Psi_{1,T} = (\varepsilon_1^T \dots \varepsilon_T^T)^T$ is the vector formed from residuals $\varepsilon_1, \dots, \varepsilon_T$ stacked together and $P_{H_{1,T}} = I_{nT} - H_{1,T} (H_{1,T}^T H_{1,T})^{-1} H_{1,T}^T$ is a projection matrix. Putting together equations (7) – (9), we get the covariance matrix of the residual ε_t :

$$\Sigma_\varepsilon = \text{cov}(\varepsilon_t) = (I_n - B) \Sigma, \quad B = \mathbb{E} [H_T (H_{1,T}^T H_{1,T})^{-1} H_T^T] \quad (10)$$

The outlet temperature model estimation should be causal because it will be used for the sequential detection of a TIB. A preliminary analysis of the real data revealed that the behavior of the temperature vector $\{Y_t\}_{t \geq 1}$ of n TCs at geometric positions (u_i, v_i) , $i = 1, \dots, n$ is non-stationary. Therefore, for this reason, the regression model (7) – (8) must be not only sequentially estimated but also permanently adapted in real-time. To avoid the computational burden, it is preferable to use the Recursive LS (RLS) algorithm to estimate/adapt the ARX (p) model given by (7) – (8). The RLS algorithm minimizes the following quadratic function of the observations (for details see [12])

$$J_T(X, A_1, \dots, A_p) = \sum_{t=1}^T \lambda^{T-t} \left\| Y_t - \tilde{H}_t X - \sum_{i=1}^p A_i Y_{t-i} \right\|_2^2 \quad (11)$$

where $0 < \lambda \leq 1$ is the forgetting factor. For the time-variant (non-stationary) system, it is necessary to have a prior model of system dynamics to design an optimal estimation algorithm. In the case of the subassembly outlet temperature, such *a priori* information is absent. For this reason, the tracking properties of the RLS is defined by a single tuning parameter λ , (for details see [12]). Usually, the forgetting factor is $\lambda \in [0.99, 0.9999]$. The RLS algorithm is defined as follows [12, 13]

$$\begin{cases} K_t &= \frac{1}{\lambda} P_t H_t^T \left(I_n + \frac{1}{\lambda} H_t P_{t-1} H_t^T \right)^{-1} \\ P_t &= \frac{1}{\lambda} (P_t - K_t H_t P_{t-1}) \\ \hat{X}_t &= \hat{X}_{t-1} + K_t (Y_t - H_t \hat{X}_{t-1}) \\ \varepsilon_t &= Y_t - H_t \hat{X}_t \end{cases}, \quad t = 1, 2, \dots, T \quad (12)$$

where the initial estimation \hat{X}_0 is assumed to be Gaussian $\hat{X}_0 \sim \mathcal{N}(X_0, P_0)$. If there is no *a priori* information available, it can be assumed that $\hat{X}_0 = 0$ and $P_0 = \gamma I_q$ with γ large.

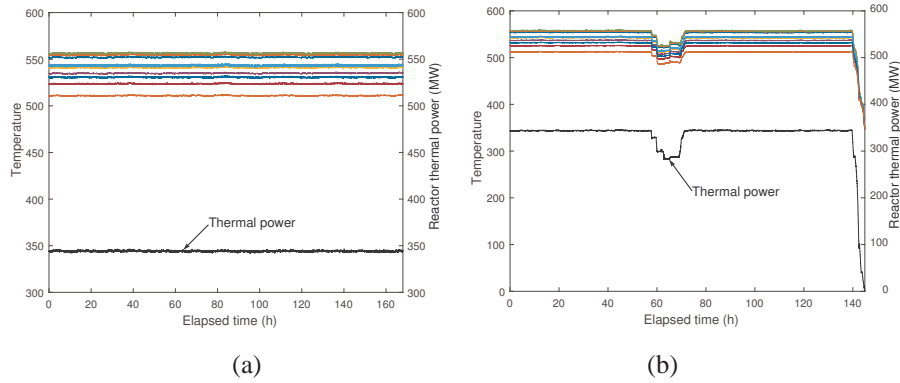


Fig. 4. **a)** The temperatures of 9 TCs (see (13)) and the reactor thermal power for the first sample covering a 7-day period from 15/02/2009 to 21/02/2009. **b)** The same parameters for the second sample covering a 7-day period from 01/03/2009 to 07/03/2009.

Let us consider a group of 9 subassemblies with the following TC numbers (see Figure 2(a))

$$23-20, 23-21, 23-22, 24-19, 24-20, 24-21, 25-18, 25-19, 25-20 \quad (13)$$

The outlet temperatures of 9 TCs (see (13)) and the reactor thermal power for two samples covering 7-day periods from 15/02/2009 to 21/02/2009 and from 01/03/2009 to 07/03/2009 are shown in Figure 4 (a) and (b). From preliminary analysis, it has been concluded that an adequate description of the outlet temperatures of a group of 9 TCs

can be done by using the order of AR-part $p = 20$. The forgetting factor λ has been chosen from the interval $[0.999, 0.9999]$.

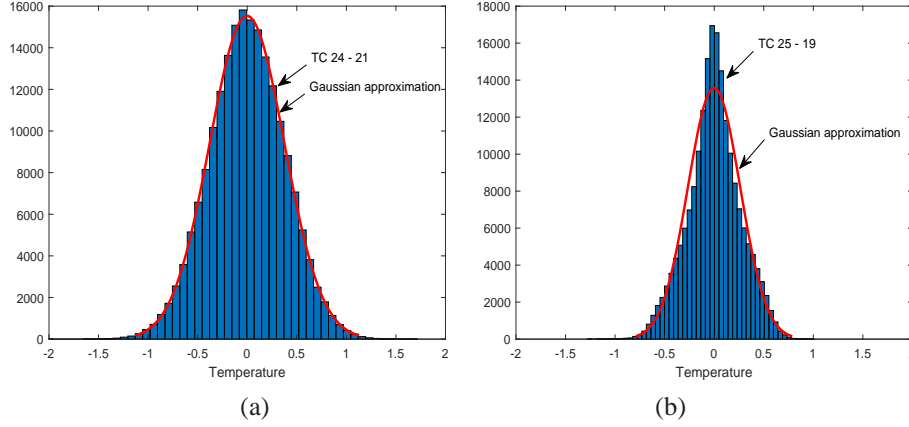


Fig. 5. **a)** The histogram of the ARX (20) model residuals corresponding to the TC 24 – 21 and its Gaussian approximation. **b)** The same parameters corresponding to the TC 25 – 19.

The role of the ARX (20) model in the TIB detection algorithm is the generation of the residuals $\{\varepsilon_t\}_{t \geq p+1}$. First of all, let us simplify the covariance matrix Σ_ε of residuals given by (10). Let $\delta = \max_{1 \leq i, j \leq n} |b_{i,j}|$, where $b_{i,j}$ is the entry in the i -th row and j -th column of the matrix B . As it follows from [12, 13], the efficient sample size T of the LS estimator using a batch of T data is given as a function of the forgetting factor λ : $T = (1 + \lambda)/(1 - \lambda)$. For the forgetting factor λ taken from the interval $[0.999, 0.9999]$, the efficient sample size T belongs to the interval $[2 \cdot 10^3, 2 \cdot 10^4]$. For such interval of T , typical values of δ obtained by using two 7-day periods of the sodium outlet temperatures belong to the interval $[10^{-2}, 10^{-3}]$. Hence, it is assumed that $\Sigma_\varepsilon \simeq \Sigma = \text{diag}\{\sigma_1^2, \dots, \sigma_n^2\}$ in the sequel.

In order to check the main statistical assumptions about the residuals $\{\varepsilon_t\}_{t \geq p+1}$ of the ARX (20) model [9, 10, 12, 13], i.e. their Gaussianity and the absence of serial and cross correlations, the following statistics have been calculated for the group of 9 TCs (see (13)):

- The histogram of the ARX (20) model residuals $\{\varepsilon_t\}_{t \geq p+1}$.
- The empirical AutoCorrelation Function (ACF) of the residuals $\{\varepsilon_t\}_{t \geq p+1}$.
- The empirical correlation matrix of the residuals $\{\varepsilon_t\}_{t \geq p+1}$.

The typical histograms of residuals (corresponding to TCs 24 – 21 and 25 – 19) are shown in Figure 5(a) and (b). The red line shows the superimposed fitted Gaussian Probability Density Function (PDF) calculated by using the empirical mean and SD. The residuals of TC 24 – 21 are better fitted to a Gaussian PDF than the residuals of TC

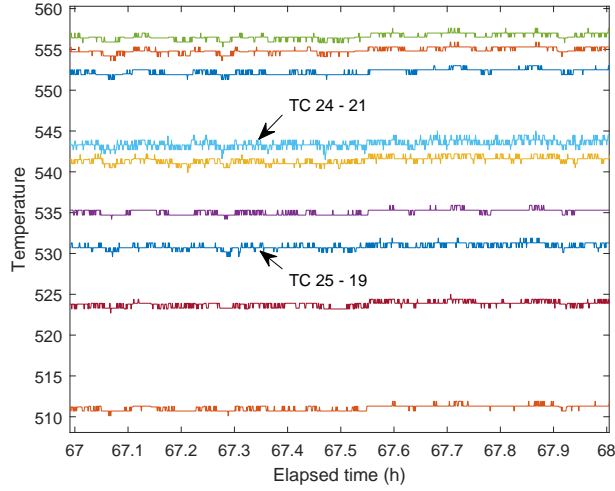


Fig. 6. A one hour registration of the temperatures of 9 TCs (see (13)).

25 – 19. This fact is explained by a relatively low resolution of 8-bit analog-to-digital converters. This situation is illustrated by Figure 6. As it follows from Figure 6, the quantization step size of some TCs is too rough w.r.t the SD of signals. The empirical ACFs of residuals are shown in Figure 7(a) and (b). As it follows from Figure 7, the empirical ACFs of residuals $\{\varepsilon_t\}_{t \geq p+1}$ look like delta-functions. Hence, the hypothesis about the absence of serial correlations seems to be likely. Finally, the empirical correlation matrix $\text{corr}(\varepsilon_t)$ of the residuals $\{\varepsilon_t\}_{t \geq p+1}$ and its determinant are

$$\text{corr}(\varepsilon_t) = \begin{pmatrix} 1.00 & 0.09 & 0.04 & 0.10 & 0.07 & 0.05 & 0.03 & 0.06 & 0.07 \\ 0.09 & 1.00 & 0.07 & 0.06 & 0.13 & 0.10 & 0.04 & 0.07 & 0.06 \\ 0.04 & 0.07 & 1.00 & 0.06 & 0.07 & 0.03 & 0.03 & 0.02 & 0.06 \\ 0.10 & 0.06 & 0.06 & 1.00 & 0.07 & 0.05 & 0.04 & 0.07 & 0.10 \\ 0.07 & 0.13 & 0.07 & 0.07 & 1.00 & 0.07 & 0.04 & 0.09 & 0.07 \\ 0.05 & 0.10 & 0.03 & 0.05 & 0.07 & 1.00 & 0.04 & 0.05 & 0.05 \\ 0.03 & 0.04 & 0.03 & 0.04 & 0.04 & 0.04 & 1.00 & 0.01 & 0.05 \\ 0.06 & 0.07 & 0.02 & 0.07 & 0.09 & 0.05 & 0.01 & 1.00 & 0.07 \\ 0.07 & 0.06 & 0.06 & 0.10 & 0.07 & 0.05 & 0.05 & 0.07 & 1.00 \end{pmatrix} \quad (14)$$

230

The non-diagonal coefficients of the matrix $\text{corr}(\varepsilon_t)$ are close to zero and $\det[\text{corr}(\varepsilon_t)] = 0.88$ is close to one. From these two facts, the hypothesis about the absence of cross-correlations between the components $\{\xi_{t,i}\}_{t \geq p+1}$ and $\{\xi_{t,j}\}_{t \geq p+1}$, where $1 \leq i \neq j \leq 9$, of the random noise $\{\xi_t\}_{t \geq 1}$ also seems to be likely.

235

Let us switch to the results of the ARX (20) model estimation. The RLS estimations (with $\lambda = 0.9995$) of the X (exogenous) and AR part coefficients as functions of

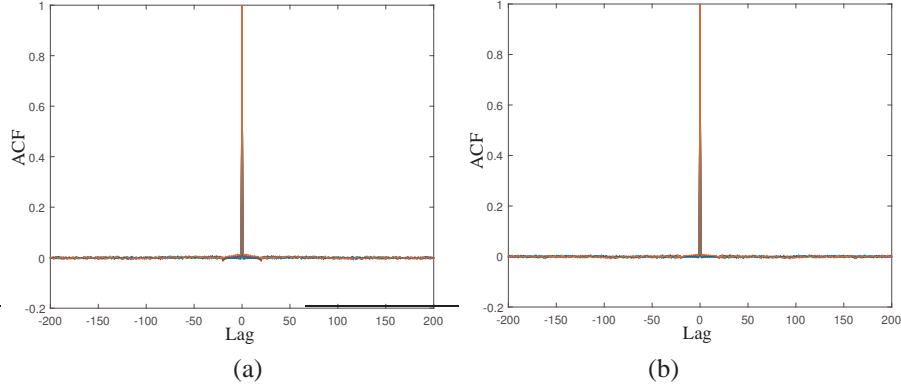


Fig. 7. **a)** The ACFs of residuals $\{\varepsilon_t\}_{t \geq p+1}$ for the group of 9 TCs (see (13)) for the first sample (15/02/2009 to 21/02/2009). **b)** The ACFs of residuals for the second sample (01/03/2009 to 07/03/2009).

elapsed time in hours are shown in Figures 8 – 9. For the AR part of the model, only the first five coefficients $\alpha_{1,i}, \dots, \alpha_{5,i}$, $i = 1, \dots, n$, calculated for TC 23 – 20, are shown in Figures 8 – 9. Other AR coefficients, $\alpha_{6,i}, \dots, \alpha_{20,i}$, $i = 1, \dots, n$, are less significant. It is clear that the variations of the RLS estimations are more important for the second sample, due to some changes in the core thermal power of the SFR, as compared to those from the first sample. It can be concluded from Figures 8 – 9 that the outlet temperatures represent strongly non-stationary signals even for a stationary operating mode of the SFR.

The crucially important parameter for the design of a TIB detection algorithm is the SD of the random noise $\{\xi_t\}_{t \geq 1}$. This parameter defines the Signal-to-Noise Ratio (SNR) in the sequel. Obviously, the true SD is unknown. For this reason, the unknown SD will be replaced with its empirical estimation. The empirical SD of the residuals $\{\varepsilon_t\}_{t \geq p+1}$ for the group of 9 TCs (see (13)) are collected in Table 1. It follows from

Sample	TC	23 – 20	23 – 21	23 – 22	24 – 19	24 – 20	24 – 21	25 – 18	25 – 19	25 – 20
First	$\widehat{\sigma}_i$	0.17	0.20	0.25	0.16	0.21	0.35	0.22	0.25	0.16
Second	$\widehat{\sigma}_i$	0.18	0.21	0.24	0.17	0.21	0.35	0.22	0.25	0.16

Table 1. The estimated SDs of the ARX (20) model residuals.

Table 1 that the residuals' SDs vary between 0.16 and 0.35. The amplitude of their variations is moderate. Hence it can be concluded that the initial hypothesis about a scalar covariance matrix $\text{cov}(\xi_{1,t}) = \sigma^2 I_{n_t}$ of the random noise $\xi_{1,t}$ is rather realistic. It is worth noting that the residuals' SDs from Table 1 correspond approximately to the random error SD obtained for the K-type TCs after a special calibration procedure for the same temperature range [14, Ch. 12], [15, Ch. 5], [16].

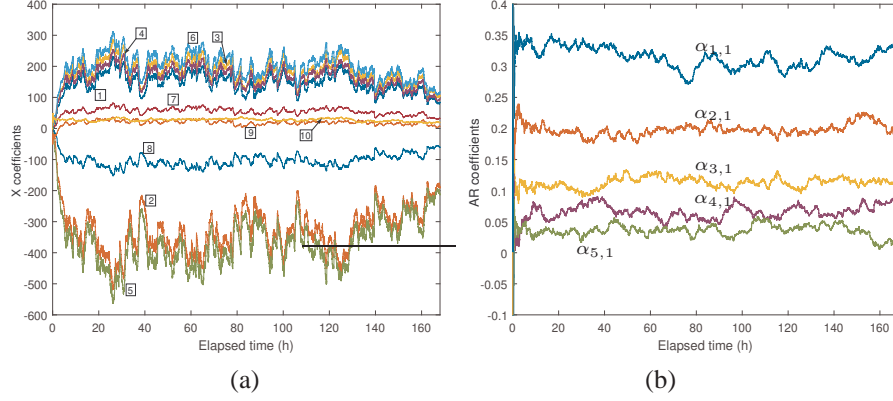


Fig. 8. **a)** The X-part coefficients (components of the vector \tilde{X} numbered from 1 to 10), calculated for the first sample (15/02/2009 to 21/02/2009). **b)** The first 5 AR-coefficients $\alpha_{1,1}, \dots, \alpha_{5,1}$, calculated for TC 23 – 20 and for the first sample (15/02/2009 to 21/02/2009).

6. Statistical detection of a single subassembly TIB

The aim of this section is to study the feasibility of early statistical detection of a single subassembly TIB. We will propose a sequential test detecting a local increase in the sodium outlet temperatures from individual subassemblies neighboring a potential TIB and calculate the probability of missed detection and the probability of false alarm provided that the delay for detection is upper bounded by a given constant for this test. The final goal is therefore to provide a complementary tool to improve the early detection of a single subassembly incident (TIB) in the context of nuclear safety.

6.1. Sequential reliable detection of abrupt changes

Let us briefly introduce the sequential detection of abrupt changes in the properties of stochastic processes [17, 18, 19, 20]. We begin with Lorden's minimax criterion of optimality [21], which involves the minimization of the (worst-case) mean detection delay provided that a prescribed level of false alarms is respected³. Let us consider the non-Bayesian framework, where the "change-point" t_0 is unknown but non-random. This non-Bayesian framework is realistic for many safety-critical systems. In opposition the Bayesian framework, it is assumed that there is no *a priori* information on the distribution of t_0 . Let $\{y_t\}_{t \geq 1}$ be a sequence of independent random variables and let t_0 be the index of the first post-change observation

$$y_t \sim \begin{cases} F_0 & \text{if } n < t_0 \\ F_1 & \text{if } n \geq t_0 \end{cases} \quad (15)$$

³The Bayesian approach to this problem and its optimal solution have been proposed by Shiryaev [22, 23].

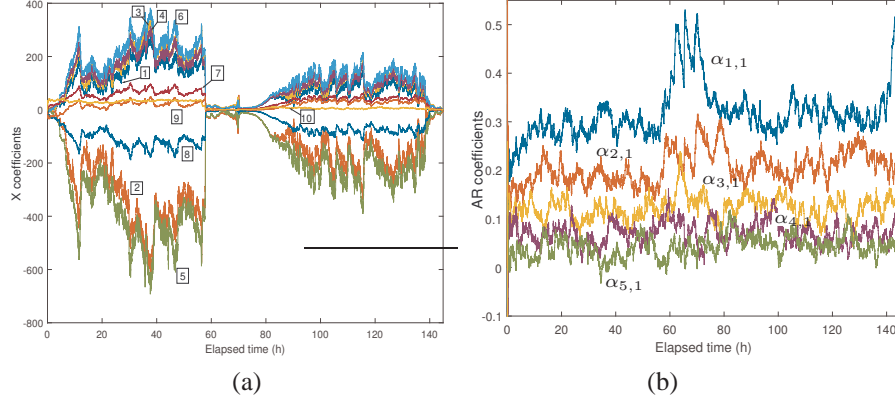


Fig. 9. **a**) The X-part coefficients (components of the vector \tilde{X} numbered from 1 to 10), calculated for the second sample (01/03/2009 to 07/03/2009). **b**) The first 5 AR-coefficients $\alpha_{1,1}, \dots, \alpha_{5,1}$, calculated for TC 23 – 20 and for the second sample (01/03/2009 to 07/03/2009).

where F_0 is the pre-change Cumulative Distribution Function (CDF) and F_1 is the post-change CDF. Let \mathcal{P}_{t_0} be the joint distribution of the observations $y_1, y_2, \dots, y_{t_0}, y_{t_0+1}, \dots$ when $t_0 < \infty$. Let \mathcal{P}_0 denote the same when $t_0 = \infty$, i.e. there is no change and all the observations y_1, y_2, \dots are i.i.d. with CDF F_0 . Let \mathbb{E}_{t_0} (resp. \mathbb{E}_0) and \mathbb{P}_{t_0} (resp. \mathbb{P}_0) be the expectation and probability w.r.t. the distribution \mathcal{P}_{t_0} (resp. \mathcal{P}_0). Lorden [21] proposed an optimality criterion, which involves the minimization of the worst-case mean detection delay

$$\inf_{T \in \mathcal{C}_\eta} \left\{ \overline{\mathbb{E}}(T) \stackrel{\text{def}}{=} \sup_{t_0 \geq 1} \text{esssup}_{\mathbb{E}_{t_0}} \left[(T - t_0 + 1)^+ | y_1, \dots, y_{t_0-1} \right] \right\} \quad (16)$$

where $(x)^+ = \max(0, x)$, $T \in \{1, 2, \dots\}$ is a stopping time w.r.t. the sequence of random variables $\{y_t\}_{t \geq 1}$, i.e. an integer random variable such that, for every $t \geq 1$, the event $\{T = t\}$ depends only on the variables y_1, y_2, \dots, y_t , among all stopping times T belonging to the class

$$\mathcal{C}_\eta = \{T : \mathbb{E}_0(T) \geq \eta\} \quad (17)$$

265 where $\eta > 0$ is a prescribed value of the Average Run Length (ARL) to a false alarm.
The traditional criterion, like (16) – (17), involves the minimization of the (worst-case) mean detection delay provided that the ARL to a false alarm is lower bounded by a given constant. It is based on the idea initially proposed by Wald [24] and motivated by the economic criteria in quality control when the price of each new observation is
270 constant. Using criterion (16) – (17), we accept that some run lengths will be very long, some other – very short, but, in the *mean*, the detection delay will be acceptable. In safety-critical applications (like a TIB detection), if the delay for detection is greater

than the required time-to-alert N , the price of each new observation is infinitely more important than the price of observation if the delay for detection is less than or equal to N . For this reason, we propose to use another criterion of reliable detection, which involves the minimization of the worst-case probability of missed detection provided that the worst-case probability of false alarm per a given reference period m_α is upper bounded.

The reliable detection of (transient) changes is motivated by two possible scenarios. The first scenario corresponds to the situation when the observed phenomena is of short and maybe unknown (and random) duration Γ . It is a so-called transient change detection problem. Sometimes even the “latent” detection (i.e. the detection after the end of transient change) is acceptable [25, 26, 27, 28, 29]. The second scenario arises when the observed anomaly (a TIB, for example) leads to serious degradation of the system performance/safety when the anomaly is detected with the delay greater than the required time-to-alert N . It is a so-called reliable detection of (transient) changes. In the framework of this second scenario, the duration Γ is assumed to be sufficient, i.e. $N \leq \Gamma$. A change detected with the delay greater than N , i.e. $T - t_0 + 1 > N$, is assumed to be missed [30, 31, 32, 33]. On the other hand, if the true duration Γ of the transient change is smaller, than the required time-to-alert N , such a transient change is considered as less dangerous because its impact on the system is limited or negligible.

Let us formalize the reliable change detection problem. We consider the sequence of random variables $\{y_t\}_{t \geq 1}$. Let t_0 be the index of the first post-change observation (unknown and non-random) and the post-change period is of sufficient duration Γ such that $N \leq \Gamma$. Let us define the generative model of the transient change for the prescribed duration N

$$y_t \sim \begin{cases} F_0 & \text{if } 1 \leq t < t_0 \\ F_{\theta_{t-t_0+1}} & \text{if } t_0 \leq t \leq t_0 + N - 1 \end{cases} \quad (18)$$

where F_0 is the pre-change CDF and $F_{\theta_1}, \dots, F_{\theta_N}$ are the known post-change distributions during the period N . It is worth noting that the transient change profile is defined only for N observations after change because all what happens after the time $t_0 + N - 1$ is considered as a missed detection.

As previously, it is assumed that \mathcal{P}_{t_0} is the joint distribution of the observations $y_1, \dots, y_{t_0}, y_{t_0+1}, \dots$ when $t_0 < \infty$. Because the considered subclass of stopping times is based on the variable-threshold truncated Sequential Probability Ratio Tests (SPRT), the existence of a short “pre-heating” period N is assumed. This short period is necessary to accumulate the first N observations y_1, y_2, \dots, y_N in order to avoid the situation when the truncated SPRT performs by using an insufficient number of observations. The quality of a statistical decision cannot be guaranteed if the number of observations is less than the required time-to-alert N , which is also equal to the minimum duration of the post-change period Γ , i.e. $N \leq \Gamma$. Finally, the optimality

criterion utilized in this report is given by [31, 32, 33]

$$\inf_{T \in C_\alpha} \left\{ \overline{\mathbb{P}}_{\text{md}}(T) \stackrel{\text{def}}{=} \sup_{t_0 \geq N} \mathbb{P}_{t_0}(T - t_0 + 1 > N \mid T \geq t_0) \right\} \quad (19)$$

where $\overline{\mathbb{P}}_{\text{md}}(T)$ is the worst-case probability of missed detection, among all stopping times $T \in C_\alpha$ satisfying

$$C_\alpha = \left\{ T : \overline{\mathbb{P}}_{\text{fa}}(T; m_\alpha) \stackrel{\text{def}}{=} \sup_{\ell \geq N} \mathbb{P}_0(\ell \leq T < \ell + m_\alpha) \leq \alpha \right\} \quad (20)$$

where $\overline{\mathbb{P}}_{\text{fa}}(T; m_\alpha)$ is the worst-case probability of false alarm during the reference period m_α measured in discrete time.

The design of the transient change detector is discussed in [31, 32, 33]. Let us briefly define this FMA test, which has been obtained as a result of optimisation in a subclass of truncated SPRT. The stopping time T_{FMA} of the FMA test is given as follows

$$T_{\text{FMA}} = \inf \{ t \geq N : \Lambda_{t-N+1}^t \geq h \}, \quad \Lambda_{t-N+1}^t = \sum_{i=t-N+1}^t \log \frac{f_{\theta_{N-t+i}}(y_i)}{f_0(y_i)} \quad (21)$$

where Λ_{t-N+1}^t denotes the Log-Likelihood Ratio (LLR) calculated for the moving window y_{t-N+1}, \dots, y_t , f_0 denotes the pre-change probability density function (PDF), $f_{\theta_{N-t+i}}$ denotes the post-change PDF and h is the threshold. In the context of a TIB detection, f_0 is the zero-mean Gaussian PDF of the ARX(p) pre-change residuals and $f_{\theta_{N-t+i}}$ is the Gaussian PDF of the ARX(p) post-change residuals.

To get upper bounds for the probabilities $\overline{\mathbb{P}}_{\text{md}}(T_{\text{FMA}})$ and $\overline{\mathbb{P}}_{\text{fa}}(T_{\text{FMA}}; m_\alpha)$ defined in criterion (19) – (20), it is necessary to respect some technical conditions and define several probabilities and their bounds. Further details and results can be found in [32, 33]. The worst-case probability of missed detection $\overline{\mathbb{P}}_{\text{md}}(T_{\text{FMA}})$ is upper bounded as follows [33]

$$\overline{\mathbb{P}}_{\text{md}}(T_{\text{FMA}}) \leq G(h) \stackrel{\text{def}}{=} \mathbb{P}_{t_0} \left(\Lambda_{t_0}^{N+t_0-1} < h \right), \quad t_0 \geq N \quad (22)$$

where $\mathbb{P}_{t_0} \left(\Lambda_{t_0}^{N+t_0-1} < h \right)$ corresponds to the probability of missed detection of the Neyman-Pearson LLR test calculated for the time window $[t_0, t_0 + N - 1]$ and the threshold h . It is assumed that the CDF of the LLR Λ_{t-N+1}^t

$$x \mapsto F(x) \stackrel{\text{def}}{=} \mathbb{P}_0 \left(\Lambda_{t-N+1}^t \leq x \right) \quad (23)$$

is a continuous function on $] - \infty; \infty[$ under the measure \mathcal{P}_0 .

The smallest value $\overline{\alpha}_1$ of the upper bound $G(h)$ provided that the upper bound for the worst-case probability of false alarm is equal to a pre-assigned value $\overline{\alpha}_0$, is given by [33]

$$\overline{\alpha}_1 = G \left[F^{-1} \left((1 - \overline{\alpha}_0)^{\frac{1}{m_\alpha}} \right) \right] \quad (24)$$

Finally, the optimal threshold is given by [33]

$$h = F^{-1} \left((1 - \bar{\alpha}_0)^{\frac{1}{m\alpha}} \right) \quad (25)$$

6.2. Rejection of nuisance parameters and adaptive detection

305 A key issue in fault detection is to state the significance of the observed deviations (e.g., a local temperature rise due to a TIB) w.r.t. random noises and nuisance parameters. Handling the presence of nuisance parameters is indeed an important issue in this framework. Distinguishing two subsets of components of the parameter vector, the parameters of interest and the nuisance parameters, is necessary because some parameters
310 of no interest for monitoring. The nuisance parameters, if not of no physical meaning, may appear in the model for its flexibility or specification, or for data interpretation reasons [34].

Let us consider a group of n TCs with a potentially accidental subassembly (TIB). We will propose a sequential test detecting a local increase in the sodium outlet temperatures of two subassemblies neighboring a potential TIB. First of all, let us define the generative model of a local increase in the sodium outlet temperatures by using equation (5) of the ARX (p) model

$$Z_t = \begin{cases} Y_t & \text{if } 1 \leq t < t_0 \\ Y_t + \theta_{t-t_0+1} & \text{if } t_0 \leq t \leq t_0 + N - 1 \end{cases}, \quad Y_t = \tilde{H}_t \tilde{X} + \sum_{i=1}^p A_i Y_{t-i} + \xi_t \quad (26)$$

where Z_t is the vector of sodium outlet temperatures measured by a group of TCs, t_0 is the TIB arrival time, $\theta_1, \dots, \theta_N$ are the vectors of additive outlet temperature
315 profiles due to a TIB, $\theta_i \in \mathbb{R}^n$. Obviously, the period of a local temperature rise due to a TIB is not limited by N but, as it follows from the criterion (19) – (20), all what happens after $t_0 + N - 1$ has no impact on the criterion of reliable change detection. For this reason, we limit the discussion to the vectors $\theta_1, \dots, \theta_N$ in the sequel. The vectors $\theta_1, \dots, \theta_N$ are parameters of interest (informative parameters) of the transient
320 change model. The vector $X = \left(\tilde{X}^T, \alpha_{1,1} \dots \alpha_{p,1} \dots \alpha_{1,n} \dots \alpha_{p,n} \right)^T$ is a nuisance parameter of this model.

An efficient method to manage the nuisance parameters and the parameter of interest is an invariant hypothesis testing approach (if the original problem is invariant) or an adaptive testing method (such as the generalized likelihood ratio test) [35, 36, 37]. Key features of these statistical methods are their ability to handle noises and uncertainties, i.e. to reject nuisance parameters, in order to decide between two hypotheses \mathcal{H}_0 (no local temperature rise due to a TIB) and \mathcal{H}_1 (there exists a local temperature rise due to a TIB). Let us go back to equation (8) and re-write it taking into account the generative model (26) with the stacked vectors $Z_{1,t}, Y_{1,t}, \xi_{1,t} \in \mathbb{R}^{nt}$ and the stacked matrix $H_{1,t}$ of size $(nt \times \ell + np)$

$$Z_{1,t} = Y_{1,t} + \theta_{1,t} = H_{1,t} X + \theta_{1,t} + \xi_{1,t} \quad (27)$$

where the stacked vector θ_1^t is defined as follows

$$\theta_{1,t} = \begin{cases} (0 \dots 0)^T & \text{if } 1 \leq t < t_0 \\ (0 \dots 0 \theta_1^T \dots \theta_{t-t_0+1}^T)^T & \text{if } t_0 \leq t \leq t_0 + N - 1 \end{cases} \quad (28)$$

where 0 is the zero row vector of appropriate size, and apply the method of invariant tests developed in [36, 37] to this regression model (27).

The idea of the invariant hypotheses testing approach is based on the existence of the natural invariance of the detection problem w.r.t. a certain group of transformation [39, Ch. 6]. In contrast to the Bayesian approach, the invariant hypotheses testing theory is based on the nuisance X rejection and, therefore, it does not use any *a priori* information on the distribution of X . It is worth noting that the drawback of the Bayesian approach in the case of a TIB detection is the following : this approach exploits some *a priori* information on the distribution of X but this information may be unreliable. Hence, the Bayesian approach is irrelevant to the case of nuisance parameters governed by an unknown environment.

The impact of nuisance parameters, expressed by the term $H_{1,t}X$ in equation (27), defines a subspace in the observation space $\mathcal{Z} = \mathbb{R}^{nt}$, i.e. the column space $R(H_{1,t})$ of the matrix $H_{1,t}$ [36, 37]. Because the unknown nuisance parameter X is non-random, the only solution is to eliminate any impact of X on the decision function. Consequently, this solution leads to a projection of $Z_{1,t}$ on the orthogonal complement $R(H_{1,t})^\perp$ of the column space $R(H_{1,t})$. The space $R(H_{1,t})^\perp$ is also well-known under the name ‘‘parity space’’ in the analytical redundancy literature [38]. It is shown in [39, Ch. 6], that the optimal invariant tests are based on the maximal invariants (principle of invariance). In the case of (27) the maximal invariant is given by the projection of $Z_{1,t}$ onto the left null space of the matrix $H_{1,t}$ (for details see [36, 37]) :

$$\Psi_{1,t} = P_{H_{1,t}} Z_{1,t} = Z_{1,t} - H_{1,t} \hat{X}, \quad \hat{X} = (H_{1,t}^T H_{1,t})^{-1} H_{1,t}^T Z_{1,t} \quad (29)$$

where $P_{H_{1,t}}$ is a projection matrix defined in (9). Hence, starting from the change-point t_0 , the observations Z_t and the matrices H_t , and $H_{1,t}$ are ‘‘contaminated’’ by the vectors $\theta_1, \dots, \theta_N$ of additive outlet temperature profiles due to a TIB.

As we have mentioned above, to design an adaptive detector of transient changes, we use the residual $\{\varepsilon_t\}_{t \geq p}$ calculated recursively by the RLS (12). Let us re-write the generative model of transient change (26) for this residual

$$\varepsilon_t \sim \begin{cases} \mathcal{N}(0, \Sigma_\varepsilon) & \text{if } 1 \leq t < t_0 \\ \mathcal{N}(M_{t-t_0+1}, \Sigma_\varepsilon) & \text{if } t_0 \leq t \leq t_0 + N - 1 \end{cases} \quad (30)$$

where $\Sigma_\varepsilon \simeq \Sigma = \text{diag}\{\sigma_1^2, \dots, \sigma_n^2\}$ is the covariance matrix of residuals and $M_{t-t_0+1} = \mathbb{E}(\varepsilon_{t \geq t_0})$ is the transient profile (expectation) of residuals due to a TIB.

Finally, let us add the following comment concerning the impact of the heteroscedasticity on the detection algorithm. As it follows from [37, Lemma 1], in the

340 case of an arbitrary covariance matrix Σ of the random noise ξ_t in the regression model (5) – (8), the LLR of the maximal invariant statistics can be calculated in two steps. The first step is a projection of $Z_{1,t}$ onto the “parity space” by using the orthogonal complement $R(H_{1,t})^\perp$ of the column space $R(H_{1,t})$ assuming that the covariance matrix Σ is scalar. The second step consists in calculating the LLR of an invariant test by
 345 using the covariance matrix of the residuals obtained after the first step. The empirical estimations of the diagonal elements σ_i^2 of this covariance matrix is given in Table 1. This means that the assumption about a scalar covariance matrix of the random noise ξ in the definitions of the LS and RLS algorithms (9) – (12) has no negative impact on the invariant statistics.

350 As it follows from Sections 4 and 5, the ARX (p) model defined by equations (5) – (8) requires a permanent adjustment to the real data due to the fact that the SFR is a time-variant (non-stationary) system. Hence, the significance of observed deviations should be established by using an adaptive estimation algorithm described in Section 5. The idea to associate a change detection algorithm to an adaptive estimation algorithm
 355 (e. g., an adaptive RLS estimator) has been considered in [40, 41, 13]. The goal of an adaptive detector of transient changes is to detect the additive outlet temperature profiles $\theta_1, \dots, \theta_N$ due to a TIB while considering the nuisance parameters as *unknown*. To solve this problem, it is proposed to use the residuals $\{\varepsilon_t\}_{t \geq p}$ calculated by an adaptive RLS estimator given by (12).

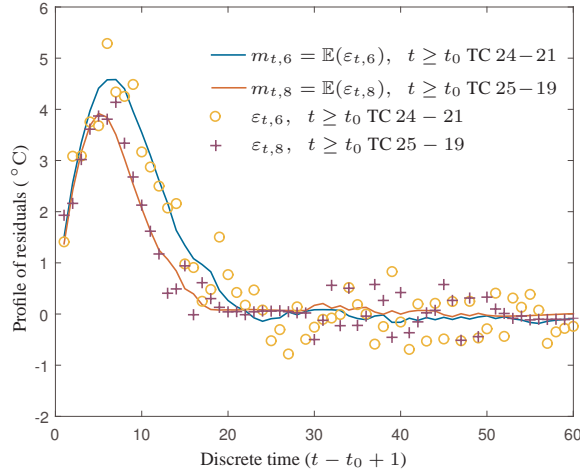


Fig. 10. The profiles of the residuals corresponding to a local increase in the sodium outlet temperatures of two subassemblies 24 – 21 and 25 – 19 neighboring a potential TIB at the subassembly 24 – 20 or 25 – 20. The rate of temperature rising is $0.5^\circ\text{C}/\text{s}$. The temperature sampling period is 3 s.

360 Let us consider the following scenario of TIB, described in [3]. It is assumed that a local increase in the sodium outlet temperatures is observed by the TCs of two

subassemblies neighboring a potential TIB beginning from the change-point t_0 . The sodium outlet temperature increases as a linear function of time. The TCs are protected by thermowells. The transfer function from the thermowell exterior temperature to the TC measurement junction is given by the first order system having a time constant of 1 s [42, Ch. 14]. Typical temperature rising profiles in the residuals corresponding to a local increase in the sodium outlet temperatures with the rate of temperature rising of 0.5°C/s are shown in Figure 10.

Let us re-write the LLR (21) of the FMA test for the sequence of residuals ε_t calculated by the RLS algorithm (12)

$$T_{\text{FMA}} = \inf \{t \geq N : \Lambda_{t-N+1}^t \geq h\}$$

$$\Lambda_{t-N+1}^t = \sum_{i=t-N+1}^t \sum_{j \in \mathcal{J}} \left[\frac{1}{\sigma_j^2} \varepsilon_{i,j} m_{i-t+N,j} - \frac{m_{i-t+N,j}^2}{2\sigma_j^2} \right] \quad (31)$$

where \mathcal{J} is a subset of TCs neighboring a potential TIB, $m_{t-t_0+1,j} > 0$ is a residual profile for $t \geq t_0$ and $j \in \mathcal{J}$. As it follows from [33] :

$$\overline{\mathbb{P}}_{\text{md}}(T_{\text{FMA}}) \leq \Phi \left(\frac{h - \frac{1}{2}d_{\mathcal{J}}}{\sqrt{d_{\mathcal{J}}}} \right), \quad \overline{\mathbb{P}}_{\text{fa}}(T_{\text{FMA}}; m_{\alpha}) \leq 1 - \left[\Phi \left(\frac{h + \frac{1}{2}d_{\mathcal{J}}}{\sqrt{d_{\mathcal{J}}}} \right) \right]^{m_{\alpha}} \quad (32)$$

where $d_{\mathcal{J}} = \sum_{j \in \mathcal{J}} \frac{\|M_j\|_2^2}{\sigma_j^2}$ is the total SNR and $\|M_j\|_2^2 = \sum_{t=1}^N m_{t,j}^2$.

6.3. Statistical properties of the sequential adaptive detector

The statistical properties of the adaptive detector defined in (31) have been examined by using :

- Asymptotic upper bounds for the probabilities of missed detection $\overline{\mathbb{P}}_{\text{md}}(T_{\text{FMA}})$ and false alarm $\overline{\mathbb{P}}_{\text{fa}}(T_{\text{FMA}}; m_{\alpha})$ given by (32).
- The sodium outlet temperatures samples covering two periods from 15/02/2009 to 21/02/2009 and from 01/03/2009 to 07/03/2009 together with two samples of the core thermal power synchronized with these temperature samples.

The non-zero components $\theta_{t,j} \in \mathcal{J}$ of the vector θ_t of additive outlet temperature rising profiles are defined as follows :

$$\theta_{t-t_0+1,j} = \kappa \Delta T (t - t_0 + 1) \text{ for } t \geq t_0 \text{ and } j \in \mathcal{J}$$

Other parameters of the TIB detection scenario are the following

$$\Delta T = 3 \text{ s}, \quad N = 3, 4, \quad m_{\alpha} = 3600/\Delta T, \quad \sigma_i \in [0.16, 0.35], \quad \lambda = 0.9995$$

The asymptotic upper bounds for the probability of missed detection $\overline{\mathbb{P}}_{\text{md}}(T_{\text{FMA}})$ are calculated as functions of the upper bounds for the probability of false alarm

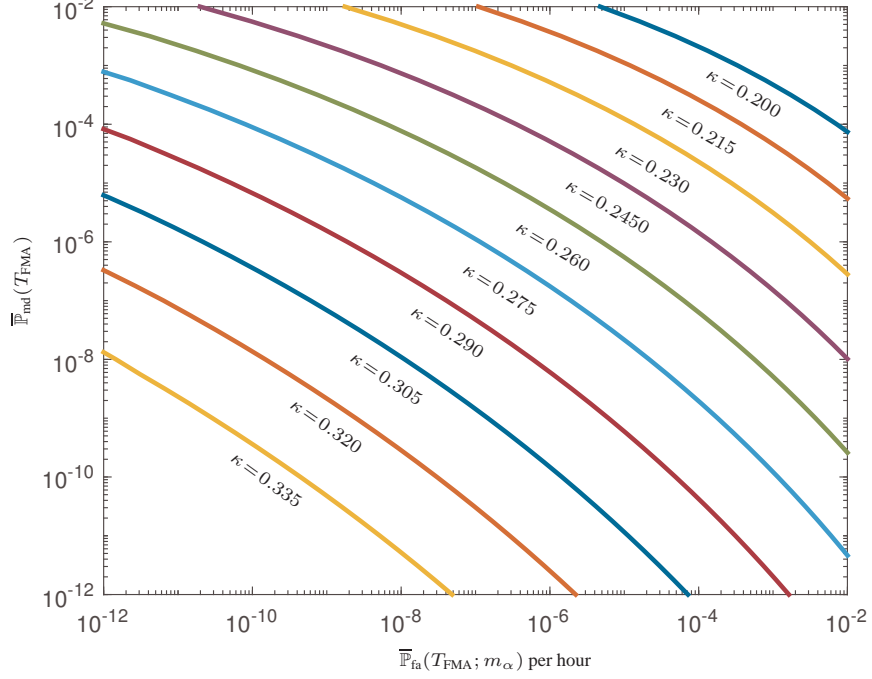


Fig. 11. The probability of missed detection $\overline{\mathbb{P}}_{\text{md}}(T_{\text{FMA}})$ as a function of the probability of false alarm per hour $\overline{\mathbb{P}}_{\text{fa}}(T_{\text{FMA}}; m_\alpha)$ for different values of the temperature rising rate $\kappa \in \{0.200, \dots, 0.335\}^\circ\text{C}/\text{s}$ for two subassemblies 24 – 21 and 25 – 19 neighboring a potential TIB at the subassembly 24 – 20 or 25 – 20. The required time-to-alert is 9 s ($N = 3$).

380 $\overline{\mathbb{P}}_{\text{fa}}(T_{\text{FMA}}; m_\alpha)$ by using equation (32). Representative curves of this function parameterized by the rate of temperature rising $\kappa^\circ\text{C}/\text{s}$ are shown in Figure 11 and 12. The results corresponding to the time-to-alert of 9 s (or $N = 3$) are shown in Figure 11 and the results corresponding to the time-to-alert of 12 s (or $N = 4$) are shown in Figure 12. It is worth noting that the probability of false alarm $\overline{\mathbb{P}}_{\text{fa}}(T_{\text{FMA}}; m_\alpha)$ is measured per hour with $m_\alpha = 3600/\Delta T$. For example, $\overline{\mathbb{P}}_{\text{fa}}(T_{\text{FMA}}; m_\alpha)$ of 10^{-5} per hour
 385 corresponds to the level of “one false alarm per $\simeq 11$ years” in mean.

The second test realized to evaluate the proposed adaptive detector defined in (31) has been done by using the sodium outlet temperature samples of 9 TCs (see (13)) covering two 7-day periods together with the corresponding samples of the core thermal power. The decision function Λ_{t-N+1}^t defined in (31) for these two samples is
 390 presented in Figure 13(a) and (b). It is assumed that the simulated TIB onset time is 120 h for both samples. The TIB location is the subassembly 24 – 20 or 25 – 20. The outlet temperature rise in the measurements of the TC 24 – 21 and TC 25 – 19 with a rising rate of $\kappa \in 0.5^\circ\text{C}/\text{s}$. The transient change profiles are shown in Figure 10. The

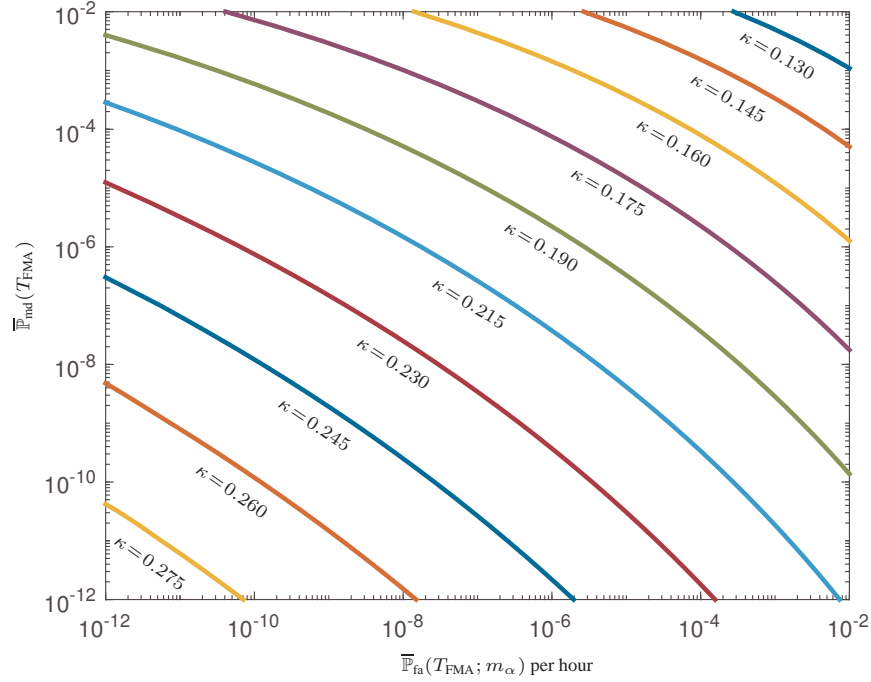


Fig. 12. The probability of missed detection $\mathbb{P}_{\text{md}}(T_{\text{FMA}})$ as a function of the probability of false alarm per hour $\mathbb{P}_{\text{fa}}(T_{\text{FMA}}; m_\alpha)$ for different values of the temperature rising rate $\kappa \in \{0.130, \dots, 0.275\}^\circ\text{C}/\text{s}$ for two subassemblies 24 – 21 and 25 – 19 neighboring a potential TIB at the subassembly 24 – 20 or 25 – 20. The required time-to-alert is 12 s ($N = 4$).

395 detection delay is 6 s for both samples; no false alarms have been reported.

7. Conclusion

This paper addresses the adaptive detection of an abnormal temperature rise due to a TIB in a single subassembly in the core of a SFR. This problem has been reduced to the reliable detection of transient changes in the residuals of a subassembly outlet temperature parametric model. The proposed adaptive recursive algorithm is composed of two parts : *i*) an adaptive RLS algorithm, which estimates the ARX (p) model of outlet temperatures measured by a local group of TCs installed at the top of the fuel subassemblies and computes the residuals of this model; *ii*) the FMA test for the reliable transient change detection, which uses these residuals to calculate the LLR in a moving window and to compare the LLR to a predefined threshold. The statistical properties of this algorithm have been studied by using the asymptotic upper bounds for the probabilities of missed detection and false alarm and by using the real data provided by the

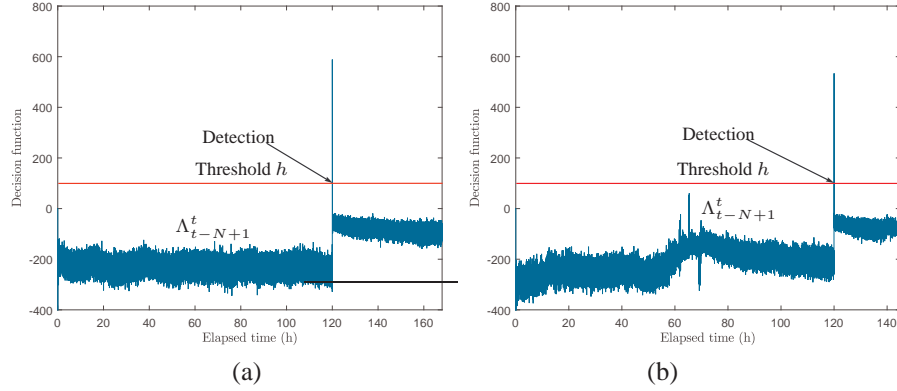


Fig. 13. **a)** The decision function Λ_{t-N+1}^t calculated for the first 7-day period from 15/02/2009 to 21/02/2009. **b)** The decision function Λ_{t-N+1}^t calculated for the second 7-day period from 01/03/2009 to 07/03/2009. The simulated TIB onset time is 120 h for both periods. The detection delay is 6 s for both periods.

center of the CEA in Cadarache.

The following conclusions and perspectives can be drawn :

- 410 • The proposed detection algorithm is recursive, numerically stable and efficient.
- If the required time-to-alert is equal to 9 s, the required probability of missed detection is upper bounded by 10^{-6} and the required probability of false alarm is upper bounded by 10^{-6} per hour, then the minimal detectable temperature rising rate in two subassemblies neighboring a potential TIB is equal to $\kappa \simeq 0.27^\circ\text{C/s}$.
- 415 If the required time-to-alert is 12 s, then the minimal detectable temperature rising rate is equal to $\kappa \simeq 0.2^\circ\text{C/s}$.
- The sampling period of temperature records used in this study is $\Delta T = 3$ s. A reduction of the sampling period ΔT to 1 s or 0.5 s can improve the statistical properties of the detection algorithm.
- 420 • Several temperature anomalies have been reported during the second 7-day period from 01/03/2009 to 07/03/2009. These anomalies are not very disturbing for the proposed TIB detection algorithm but it can be interesting to examine this phenomena carefully in the case of a future study.
- Several hundred (thousand) local groups of TCs have to be monitored simulta-
425 neously to cover a fuel assembly. It is interesting to compute the probability of false alarm for such a stream of parallel data in the case of a future study.

8. Acknowledgements

The authors gratefully acknowledge the research and financial support of this work from the Commissariat à l'Énergie Atomique et aux Énergies Alternatives (CEA), from
430 the group of scientific interest GIS 3SGS, and from the project AAP NEEDS of CNRS, France.

References

- [1] Nomoto, S., Yamamoto, H., Sekiguchi, Y., Tamura, S. (1980) Measurement of subassembly outlet coolant temperature in the JOYO experimental fast reactor, Nuclear Engineering and Design, Vol. 62, Issues 1–3, 1980, pp. 233–239.
435
- [2] Chellapandi, P., Velusamy, K. (2015) Thermal hydraulic issues and challenges for current and new generation FBRs, Nuclear Engineering and Design, Vol. 294, 2015, pp. 202–225,
- [3] Paumel, K., Jeannot, J.P., Jeanne, T., Laffont, G., Vanderhaegen, M., Massacret, N. (2013) R&D on early detection of the Total Instantaneous Blockage for 4 th Generation Reactors – inventory of non-nuclear methods investigated by the CEA. In the Proceeding of the 3 rd International Conference on Advancements in Nuclear Instrumentation, Measurement Methods and their Applications (ANIMMA), 23-27 June 2013, Marseille, France.
440
- [4] Sarkar, M., Velusamy, K., Munshi, P., Singh, O.P. (2018) Investigation of heat transfer from a totally blocked fuel subassembly of fast breeder reactor with 7 and 19 pin bundles. Nuclear Engineering and Design, vol. 338, 2018, pp. 74–91.
445
- [5] Straka, M. (1978) Some techniques for computerized LMFBR - subassembly outlet temperature monitoring based on estimation theory. In the Proceeding of the Fourth IFAC International Symposium on Multivariable Technological Systems, Fredericton, Canada, 4-8 July 1977, Published for the IFAC by Pergamon Press, Oxford; New York: December, pp. 483–488
450
- [6] Hartert, L., Nuzillard, D., Jeannot, J.P. (2013) Dynamic detection of nuclear reactor core incident, Signal Processing, vol. 93, Issue 2, 2013, pp. 468–475,
- [7] Martinez-Martinez, S., Messai, N., Jeannot, J.P., Nuzillard, D. (2015) Two neural network based strategies for the detection of a total instantaneous blockage of a sodium-cooled fast reactor, Reliability Engineering & System Safety, vol 137, 2015, pp. 50–57
455
- [8] Jeanne, T. (1990). Modélisation des transferts thermiques par conduction et rayonnement, dans une géométrie quelconque, multicomposant en multiphase, Thèse en Énergétique, Université de Provence (Aix-Marseille 1).
460

- [9] Box, G., and Jenkins., G. (1970) *Time Series Analysis : Forecasting and Control*. Holden-Bay, San Francisco.
- [10] Anderson, T.W. (1971) *The Statistical Analysis of Time Series*. Wiley & Sons,
465 New-York.
- [11] Brillinger., D.R. (1981) *Time Series, Data Analysis and Theory*. Rinehart & Winston, New-York.
- [12] Ljung, L., and Söderström, T. (1985) *Theory and practice of recursive identifica-
tion*. MIT Press series in signal processing, optimization, and control, 529 p.
- 470 [13] Gustafsson, F. (2000) *Adaptive Filtering and Change Detection*. John Wiley & Sons, Ltd, 500 p.
- [14] ASTM Committee E-20 on Temperature Measurement (1981) *Manual on the Use
of Thermocouples in Temperature Measurement*. American Society for Testing & Materials, 275 p.
- 475 [15] Childs, P. (2001) *Practical Temperature Measurement*. Butterworth-Heinemann, 368 p.
- [16] Nakos, J. T. (2004) *Uncertainty Analysis of Thermocouple Measurements Used
in Normal and Abnormal Thermal Environment Experiments at Sandia’s Radiant
Heat Facility and Lurance Canyon Burn Site*. Sandia National Laboratories, Albu-
480 querque, New Mexico 87185 and Livermore, California 94550, 82 p.
- [17] Basseville, M. and Nikiforov, I.V. (1993). *Detection of Abrupt Changes: Theory
and Application*. Prentice Hall, www.irisa.fr/sisthem/kniga.
- [18] Lai, T.L. (2001). Sequential analysis : some classical problems and new chal-
lenges (with discussion). *Statistica Sinica*, 11, 303–408.
- 485 [19] Poor, H. and Hadjiliadis, O. (2009). *Quickest detection*. Cambridge University Press.
- [20] A. Tartakovsky, I. Nikiforov, and M. Basseville, *Sequential Analysis : Hypothesis
Testing and Changepoint Detection*. CRC Press, Taylor & Francis Group, 2014.
- [21] Lorden, G. (1971). Procedures for reacting to a change in distribution. *The Annals
490 of Mathematical Statistics*, 42(6), 1897–1908.
- [22] Shiryaev, A.N. (1961). The detection of spontaneous effects. *Soviet Mathemat-
ics – Doklady*, 2, 740–743. Translation from Doklady Akademii Nauk SSSR,
138:799–801, 1961.
- 495 [23] Shiryaev, A.N. (1963). On optimum methods in quickest detection problems. *Theory of Probability and its Applications*, 8(1), 22–46.

- [24] A. Wald, (1947). *Sequential Analysis*, ser. Dover Phoenix Editions. Dover Publications, 2004. [Online]. Available: <http://books.google.fr/books?id=oVYDHHzZtdIC>
- [25] C. Han, P. K. Willett, B. Chen, and D. A. Abraham, “A detection optimal min-max test for transient signals,” *IEEE Trans. on Information Theory*, vol. 44, no. 2, pp. 866–869, Mar. 1998.
- [26] R. Streit and P. Willett, “Detection of random transient signals via hyperparameter estimation,” *IEEE Trans. Signal Process.*, vol. 47, no. 7, pp. 1823–1834, Jul. 1999.
- [27] C. Han, P. Willett, and D. Abraham, “Some methods to evaluate the performance of Page’s test as used to detect transient signals,” *IEEE Trans. Signal Process.*, vol. 47, no. 8, pp. 2112–2127, Aug. 1999.
- [28] Z. Wang and P. Willett, “A performance study of some transient detectors,” *IEEE Trans. Signal Process.*, vol. 48, no. 9, pp. 2682–2685, Sep. 2000.
- [29] Z. J. Wang and P. Willett, “A variable threshold Page procedure for detection of transient signals,” *IEEE Trans. Signal Process.*, vol. 53, no. 11, pp. 4397–4402, 2005.
- [30] Bakhache, B. and Nikiforov, I. (2000). Reliable detection of faults in measurement systems. *International Journal of Adaptive Control and Signal Processing*, 14(7), 683–700.
- [31] Guepie, B., Fillatre, L. and Nikiforov, I. (2012). Sequential Monitoring of Water Distribution Network. In the Proceeding of the SYSID 2012, 16th IFAC Symposium on System Identification, Brussels, Belgium, July 11-13.
- [32] Guépié B. K., Fillatre L., and Nikiforov, I. (2012). Sequential detection of transient changes. *Sequential Analysis*, vol. 31, no. 4, pp. 528–547.
- [33] Guépié, B. K., Fillatre, L. and Nikiforov, I. (2017) Detecting a suddenly arriving dynamic profile of finite duration. *IEEE Trans. on Information Theory*, vol. 63(5), 3039–3052.
- [34] Basseville, M. and Nikiforov, I. (2005) Handling nuisance parameters in systems monitoring. In the Proceedings of the 44th IEEE Conference on Decision and Control, and the European Control Conference 2005 Seville, Spain, December 12-15, pp. 3832–3837.
- [35] Scharf, L.L., Friedlander B. (1994) Matched Subspace Detectors. *IEEE Trans. Sign. Proc.*, vol. 42, no. 8, pp. 2146–2157, August.
- [36] Fouladirad, M., Nikiforov, I. (2005) Optimal statistical fault detection with nuisance parameters, *Automatica*, vol. 41, Issue 7, pp. 1157–1171.

- [37] Fouladirad, M., Freitag, L. Nikiforov, I. (2008) Optimal fault detection with nuisance parameters and a general covariance matrix, *Int. J. Adapt. Control Signal Processing*, vol. 22, pp. 431–439.
- [38] Frank, P. M. (1990) Fault diagnosis in dynamic systems using analytical and knowledge-based redundancy: A survey and some new results, *Automatica*, vol. 26, Issue 3, pp. 459–474.
- [39] E. Lehmann and J. Romano, *Testing Statistical Hypotheses*, ser. Springer Texts in Statistics. Springer, 2005. [Online]. Available: <http://books.google.fr/books?id=Y7vSVW3ebSwC>
- [40] Benveniste, A., Basseville M., and Moustakides, G. (1987) The asymptotic local approach to change detection and model validation. *IEEE Transactions on Automatic Control*, vol. 32, no. 7, pp. 583–592, July.
- [41] Benveniste, A., Metivier, M., and Priouret, P. (1990). *Adaptive Algorithms and Stochastic Approximations*, Springer-Verlag Berlin Heidelberg, 365 p.
- [42] Bentley, J.P. (2005) *Principles of Measurement Systems*, Pearson Prentice Hall, 528 p.